IJE TRANSACTIONS C: Aspects Vol. 35 No. 12, (December 2022) 2395-2402

International Journal of Engineering

Journal Homepage: www.ije.ir

Numerical and Experimental Investigation on Small Scale Magnetorheological Damper

S. Vivekananda Sharma*, G. Hemalatha

Department of Civil Engineering, Karunya institute of technology and Sciences, Coimbatore, India

P A P E R I N F O

Paper history:
Received 24 August 2022
Received in revised form 22 September 2022
Accepted 23 September 2022

Keywords:
COMSOL
Finite Element Method
Excitation Frequency
Servo-Hydraulic UTM
Material Testing Machine Suite
Damping Force
Vibration Control
Civil Application

A B S T R A C T

This paper presents the design of an Magnetorheological (MR) damper that includes an arrangement of a piston and cylinder. This study developed a 3-D model based on the finite element method (FEM) concept on the COMSOL Multiphysics to analyze and investigate the MR damper characteristics. A prototype of the MR damper is being fabricated based on the FEM model and is put through a series of experiments using the Servo-Hydraulic material testing machine (MTS). Maximum and minimum forces, 171.5235N and 249.2749N, were measured at 0.1Hz and 1Hz, respectively, for the FEM model. The fabricated model obtained similar results at 0.1Hz and 1Hz, with maximum and minimum forces of 175.9103N and 252.7765N, respectively. Comparing these two model analyses reveals that the FEM-based model accurately depicts the experimental behaviour of the MR damper in terms of its damping force, although there is minor variation. The findings of this paper will be helpful for designers in creating MR dampers that are more efficient and reliable, as well as in predicting the characteristics of their damping force.

***doi**: 10.5829/ije.2022.35.12c.16*

NOMENCLATURE

F_τ	Yield stress force(N)	Q	volumetric flow rate (mm^3/s)
F_η	Viscous Component force(N)	A_p	C/s of piston area ($mm^{2)}$
F_f	Friction Component force(N)	D	Diameter of cylinder (mm)
F_D	Total damping force(N)	d_o	Diameter of piston Rod (mm)
v	velocity of the piston (mm/s^2)	h	Height of piston (mm)
L_t	Length of Piston rod (mm)		
Greek Symbols			
τ_y	Shear stress(kPa))	ω	circumference of the flow path
η	Viscosity of MR fluid	$Sgm(\upsilon)$	reciprocating motion
β	Magnetic Field density (T)		

1. INTRODUCTION

Engineers and researchers aim to learn vibration control technology since civil infrastructure, automotive systems, and industrial equipment vibrate excessively. Magnetorheological dampers,as a method of vibration control technology are used to stop excessive vibrations. It's an improved version of hydraulic damper. Magnetorheological fluid has been replaced with damper oil (MR fluid). This MR fluid contains carrier liquid and freely movable magnetic particles. MR fluid operates like damper oil without magnetic fields. Iron particles in a magnetic field generate a chain pattern. This structure dampens extrinsic vibrations in the electromagnetic field created by an electromagnet on the damper piston. Electromagnets have many copper coils and electrifying the coils creates an electromagnetic field. Shaking buildings use MR dampers as a semi-active control system. The MR damper was popular with researchers because it is controllable and used little electricity. This allowed it to reduce the vibrations in buildings. Magnetorheology is based on how a magnetic field

*Corresponding Author Institutional Email:
svivekananda@karunya.edu.in (S. Vivekananda Sharma)

Please cite this article as: S. Vivekananda Sharma, G. Hemalatha, Numerical and Experimental Investigation on Small Scale MR damper, ***International Journal of Engineering, Transactions C: Aspects***, Vol. 35, No. 12, (2022), 2395-2402

affects fluid rheology. Magnetic fields abruptly modify viscosity (in a few milliseconds) [1]. Magnetorheological fluid is created by combining a carrier liquid with ferromagnetic particles and additives. Ferromagnetic particles float freely in the absence of a magnetic field. Ferromagnetic particles account for 20-40% of total volume (25 to 80 percent by weight). A magnetic field is absent, whereas the presence is ON. In the ON state, ferromagnetic particles form a chain due to the magnetic field. MR damper has a strong damping force with a low magnetic field. The research needs to consider the damper's dynamic performance as a result of the various loading situations, stroke length, current input, and other factors [2].

The MR damper is most commonly used in the suspension of motor vehicles; however, its application has recently been expanded to include other critically important structures, like buildings, turbines, wind bridges, washing machines, prosthetic limbs, landing gear, and so on [3-9].

Srinivasan et al. [10] studied many different magnetorheological (MR) damper valve designs and analyzed their performance indices. These performance parameters included inductive time constant, valve ratio, dynamic range, and pressure drop. To reduce the risk of earthquakes, Daniel et al. [11] concentrated on the issue of adjusting the damping force of a shear mode magnetorheological damper. Consequently, the MR damper operating in shear mode capable of controlling vibration is studied using experimental and computational methods. Seid et al. [12] designed and analyzed an above-knee prosthesis using a magnetorheological (MR) damper. A dynamic system model for the prosthetic leg swing phase with a single-axis knee and optimal MR damper was created. The research was carried out by Hou et al. [13] to investigate the performance of an MR damper after it had been mounted on a material testing machine (MTS) and put through a series of tests with varied excitation frequencies. The reaction time parameters, energy dissipation, and responsive force were analyzed in this research. The results of the experiments served as the basis for these analyses. Wu and Cai [14] discovered in their research that MR dampers regulate the vibrations of cable-stayed bridges under various excitation frequencies, one of which is the resonant frequency. When constructing twin-tube MR dampers that are outfitted with a single coil, it is common to practice using magnetic shields and sandwiched magnetic shields. This research was conducted by Ganesha et al. [15] and concluded that the experiment was successful, as evidenced by improvements in suspension control, ride comfort, and deflection of tires.

Wani et al. [16] suggested two response-based-adaptive control techniques for reducing inter-story drift and acceleration response. Control techniques are combined with the device location algorithm to determine the optimal magnetorheological damper configuration and controls system design parameters. Fast Fourier transform response showed that the structure's reactionwas attenuated and spread throughout its modes.

Wani et al. [17] measured the in-plane motion of a five-story steel structure on a shake table using magnetorheological dampers (MR). Measurements of displacement, velocity, acceleration, displacement, story drift of the floors, and stresses in base column are collected and compared with standard data. The shake table results showed the efficiency and precision of the proposed DIC system in monitoring structural responses compared to noisy responses, highlighting the potential of this technique for monitoring, controlling, and reconnoitring a wide range of structures during and after extreme events. Daciel et al. [18] built a 10kN MR damper with an RCC frame. This frame was earthquake-excited at 0 A, 3 A, and without an MR damper for comparison. Comparisons showed displacement reductions, force increases, and crack pattern modifications. The suggested semiactive damper can reduce structural responses in moderate to high seismicity locations. Daciel et al. [19] studied which includes designing, developing, and testing a novel MR damper. Multi-coil magnetic generating was employed to boost flow gap shear force. The research examines the proposed system's element and structure-level reactions to strong ground motions. OpenSees was used to simulate a building structure to demonstrate its usefulness.

Abdeddaim et al. [20] improved SSI between a based isolated structure and soil with an MR damper. Using 100 earthquake arrays, the structure's dynamic behaviour was studied. The results showed that optimising base-isolated structures with an MR damper improved their response. Rashid et al. [21] examined a 5-story steel frame employing an ARBA method paired with a device placement optimization technique and an MR damper control system. The numerically simulated results demonstrated that MR damper locations are highly correlated to the designer's output aim. ARBA approaches outperformed uncontrolled and passive control systems in modulating the structure's acceleration response and improved dynamic serviceability. Wani et al. [22] conducted computational and experimental research to determine the efficiency and performance of a suggested MRO-based control with iterative technique using magnetorheological (MR) dampers as a control device in reducing structural reaction. Results showed the strategy's effectiveness and versatility in minimising structural responses. The control tactics were then tested on a five-story steel frame with an MR damper. The results showed MRO control is superior to passive control in minimising structural reactions.

Wani et al. [23] studied structure arrangement and damper number on response decrease. In this study, one and two MR dampers at different stories are used to evaluate the control of a five-story structure based on performance metrics. It also introduced a fail-safe current value for each floor's MR damper in case of feedback or control failure. The results suggested placing dampers on the ground floor, then the second, and lower-floor MR dampers should have a greater failsafe current value for effective passive control of the structures.

In this paper,as an extension work of Vivekananda et al. [24], a three-dimensional model employing the finite element approach is developed again by making use of the effective parameters [24] using COMSOL Multiphysics (FEM). Based on this information, the damping force obtained through computational and experimental analysis is validated for the model after the fabricated MR damper has been tested in the servo-hydraulic MTS.

2. ANALYSIS OF SMALL-SCALE MR DAMPER USING FEM

In order to simulate the behavior of a physical system or assembly, FEM breaks down a physical system or assembly's geometry into a large number of small, uniformly shaped elements, formulates equations, applies loads and constraints to the boundary conditions, and then solves the modified system equations for the relevant unknown field variables, such as strain, temperature, magnetic flux, and displacement. This work uses the widely-used FEM COMSOL Multiphysics software[1].

The study of the MR damper is an interesting and potentially gainful endeavor because it enables a controllable damping force to be generated simply by adjusting the current that flows through its coil (Figure 1). The current can be induced through a DC power supply, motor vehicle batteries, or a normal battery. With the aid of the finite element method, various researchers aim to model and design MR dampers from various design perspectives (FEM). Consequently, various MR dampers designs have emerged, each featuring a operating principle, effective range and unique geometry [25]. An MR damper's damping force depends on the magnetic field induced in the piston-cylinder clearance [26]. Figure 2 depicts the magnetic circuit of the MR damper, which was derived from a comprehensive review of the relevant literature. The MR damper is modeled with the parameters listed in Table 1.

[1] https://doc.comsol.com/5.4/doc/com.comsol.help.acdc/ACDCModuleUsersGuide.pdf

2. 1. Modelling of MR damper in COMSOL To conduct static magnetic analysis of the MR damper using the COMSOL Multiphysics. the following steps are taken.

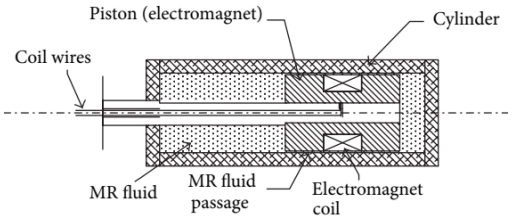

Figure 1. Schematic of MR Damper

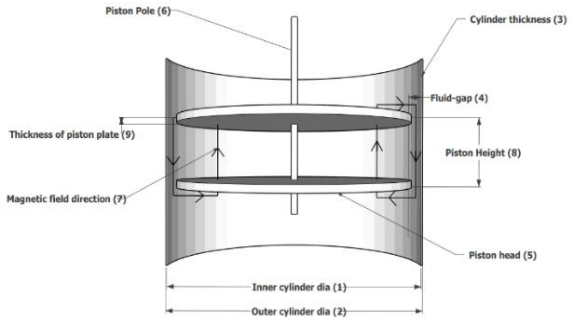

Figure 2. Flow diagram of Magnetic circuit in MR damper

TABLE 1. Dimensions of MR Damper's Prototype

Parameter	Dimension
(1) Inner Cylinder Dia	40mm
(2) Outer Cylinder Dia	44mm
(3) Cylinder Thickness	2mm
(4) Annular Fluid Gap	1mm
(5) Piston plate Dia	38mm
(6) Piston rod Dia	10mm
(8) Piston Height	50mm
(9) Piston plate Thickness	5mm

TABLE 2. MRF 132DG Properties

Properties	132DG MRF
Density	2.44 gm/cm3
Flash-Point	>170
Yield-Stress	47 kPa
Solid/Weight ratio	72
Working Temp.	-15 to 160 Celcius
Responsive time	Less than Millisecond
Viscosity	0.28(pa.s)@40oC

a) Building Physical Environment
b) Add physics properties to specific regions, and Build and mesh the model.
c) Excite boundary conditions and loading conditions.
d) Obtain solutions
e) Simulate and post-processing of results

The MR damper is an axisymmetric solid that is being stressed in an axisymmetric manner. Keeping in mind that a 2D FEM simulation is sufficient for the simulation, the 3D model has opted in this work as not much literature is available on using the 3D prototype, as presented in Figure 3. The cylinder, piston, and MR fluid annular gap are static components of the electromagnetic coil's magnetic circuit. In COMSOL modeling, 500 coil turns are utilized to measure magnetic flux density. Variable coil current produces variable magnetic flux density. As for this specific model, cylinder and piston material is adopted as steel with the relative permeability value as 2000 Coil relative permeability as 1, MR fluid as 6, and free space's magnetic permeability as $4\pi \times 10^{7}$ H/m [26].

2. 1. 1. Physics Environment Space requires a 3D model. The Solid Works model is loaded into COMSOL as a step file. Figure 4 shows the air-encased model. Determining the magnetic field induced by coil current flow is the issue. COMSOL Multiphysics AC/DC interface is used. Next, the issue analysis includes magnetic fields (mf) physics. Magneto-static analysis enables for stationary examination[1].

2. 1. 2. Material Attribution Magnetic fields in the air are explored using a 3D model. The piston rod and head are made of mild steel. The electromagnetic coil uses solid copper. Inner and outer piston poles are made of mild steel. MR fluid gap incorporates Lord Corporation's MRF 132DG fluid specifications. Table 3 lists 132DG MR fluid's properties[2].

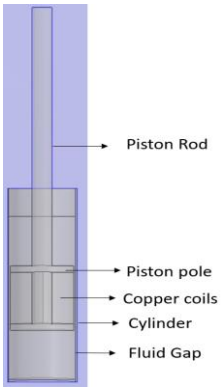

Figure 3. 3D model of MR damper in COMSOL

2. 1. 3. Meshing Figure 4 shows the generated mesh using ultra-fine meshing in the physics-controlled domain. 8 domains, 84 edges, and 48 vertices make up the mesh model. The extreme mesh for simulation includes 10,18,846 elements, including 1,02665 border elements and 3,624 edge elements [24].

2. 1. 4. Boundary Conditions The model's center plane is axisymmetric. Using a magnetic insulation boundary condition (air medium), the full domain's outside boundaries can be applied, provided no flux leakage beyond the work area. In COMSOL, the coil area refers to the boundary condition of the coil wire, which has a C/S area of 0.2192mm^2, or Copper wire SWG 16. Every 0.5A simulation increases the coil's current by 0.5A to 2A. The domain, excluding the coil, is subject to ampere law[3].

2. 1. 4. Solving Time-independent stationary magnetostatics solves the problem. The problem is solved using COMSOL's Magnetic fields module. This module solves Maxwell's equations according to specified boundary conditions using a laptop with an AMD Ryzen 5 2500u processor with 4 central cores and 8 secondary cores and a base clock speed of 2.3 GHz, which is more than enough to carry out the study. Simulation solved 79,21,037 SDOF. The MUMPS solver in COMSOL Multiphysics solves the simulation using 1 as tolerance and 1000 as residual [24]. This simulation varied current and coil turns.

2. 1. 5. Post-processing of Result COMSOL Multiphysics can show flux density flow lines in 2D as surface and in 3D as volume. Through the MR fluid gap, magnetic flux lines flow over the working domain. Between the outer and inner poles, flux lines jump. The MR fluid gap between the inner and outer poles has the most flux lines. Near the magnetic coil, the MR fluid gap exhibits few flux lines. Figure 5 shows the 3D flux density distribution. We can get the desired outcomes by adjusting the current input and coil count.

3. DAMPING FORCE CALCULATION

The magnetic flux densities computed by the COMSOL are used to determine the MR damper's damping force for

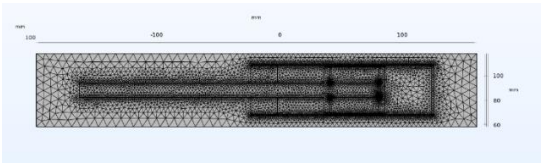

Figure 4. The extrafine meshing of model

[1] https://doc.comsol.com/5.4/doc/com.comsol.help.acdc/ACDCModuleUsersGuide.pdf

[2] www.lord.com (https://www.lord.com/sites/default/files/Documents/TechnicalDataSheet/DS7015_MRF-132DGMRFluid.pdf)

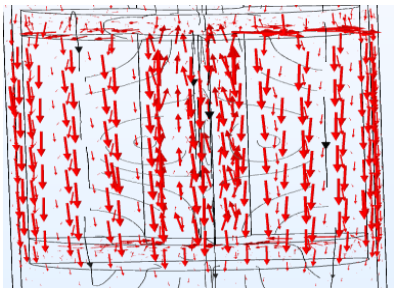

Figure 5. Magnetic Flux lines

the FEM model. For this purpose, the graphs provided by the Lord Corporation, USA, are used to develop the relationship between the shear stress (τ_y) and the magnetic flux density (B) for Lord MRF-132DG.

The final equation is displayed in Equation (1). The value of shear stress procured at specific magnetic flux levels is then used to calculate the damping force in Equation (5).

$$\tau_y = (6.9 * 10^2) + (4 * 10^4)\beta - (1 * 10^5)\beta^2 + (9.1 * 10^4)\beta^3 \quad (1)$$

Induced yield stress, denoted by F_τAnd viscous components, denoted by F_η They are said to be the components that make up the damping force, F_D, in accordance with the Bingham plastic model [26-28] of plates. This is illustrated as:

$$F_D = F_\tau + F_\eta$$

$$F_D = \left[\left(2.07 + \frac{12Q\eta}{12Q\eta + 0.4\omega h^2 \tau_y}\right) \times \frac{\tau_y L A_p}{h}\, Sgm(v)\right] + \left[\left(1 + \frac{\omega h v}{2Q}\right) \times \frac{12Q\eta L_t A_p}{\omega h^3}\right] \quad (2)$$

where,

$$Q = A_p \times v \quad (3)$$

$$A_p = \frac{\pi}{4}\left(D^2 - {d_o}^2\right) \quad (4)$$

Q represents the rate of volumetric flow rate of the MR fluid, A_P represents the C/s of piston area, D represents the diameter of cylinder and d_0 represents the diameter of the piston rod, v represents the velocity of the piston, τ_y represents the shear yield strength of the MR fluid, η represents the viscosity without excitation, L_t represents the pole length, ω represents the mean circumference of the flow path of the damper, h represents the height of piston and $Sgm(v)$ represents the reciprocating motion of the piston.

According to the researchers [29-31] one must take into account the system's frictional forces (F_f). Considering friction is prevalent on the contact area of both the movable and the stationary components of the MR damper, it is unwise to ignore it in the study. The total damping force is represented as F_D

$$F_D = F_\tau + F_\eta + F_f \quad (5)$$

Using the Equations (1) to (5), damping force of the piston is computed numerically and presented in Table 4.

4. EXPERIMENTAL SETUP

Using the dimensions chosen in Table 1 for Finite element modeling, a prototype MR damper is constructed. Figure 6 depicts the whole assembly of the prototype MR damper's component pieces. The clearance area between the piston and cylinder in the damper allows MR fluid to flow from a higher to lower chamber and, conversely, when the piston starts moving.

Using the LORD MRF-132DG in the MR damper, the prototype magnetorheological damper is evaluated for performance using the MTS. Figure 7 represents the Servo-Hydraulic MTS setup used for the experimental analysis.

The MTS constitutes a power unit capable of exciting frequency for a range of 0.1 to 2 Hz and a rated sine force of 1000 kN. The MTS has a 127 mm peak-to-peak amplitude rating. The vibration's amplitude is adjusted at a desirable value by changing the test system's displacement input and excitation frequency. MTS can be controlled both manually or through a system-based

Figure 6. Fabricated MR damper

Figure 7. MTS setup

control mode. Only vertical vibrational analysis may be performed with the shaker. MTS Suite controls system is a system-based controller with a built-in signal recorder.

The MTS suite is programmed to collect real-time data and provides real-time data in time, acceleration, displacement, velocity, and force. The damper is positioned vertically in the loading frame of MTS, as shown in Figure 8, which is also a part of the testing system.

For safety, the MR damper's piston beginning position is managed using the control system or manually. Before the MR damper's experimental performance examination, the piston is placed in the cylinder's center.

The test is run at a fixed displacement of 10 mm for 10 cycles. Repeating the test under the same circumstances with a different frequency and supplying a steady 2A current to the MR damper's electromagnetic coil. The MTS suite control system monitors the force for every test run.

4. RESULTS

The magnetic flux density generated according to COMSOL, increases with induced MR damper current. Figure 9 and Table 3 quantify these phenomena, and the effect of magnetic flux density on the piston area is also observed.It is evident from Figure 9 , how the increase in current input leading to increase in magnetic flux affects the piston area.

Figure 8. MR damper on the MTS loading frame

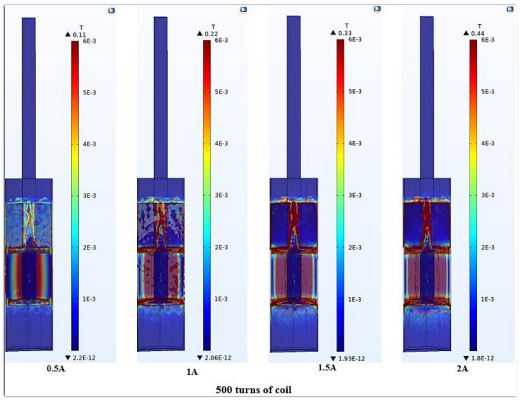

Figure 9. Effect of magnetic flux on the piston area

TABLE 3. Magnetic flux density procured using the FEM model

Input Current(A)	Magnetic Flux Density (Tesla)
0.5A	0.11T
1A	0.22T
1.5A	0.33T
2A	0.44T

The experimental damping force, displacement, and velocity acquired by the piston rod are recorded by the MTS suite's built-in DAQ system. The experimental damping force that was achieved for various stimulation frequencies is given in Table 4. This damping force is contrasted with the outcomes of the numerically procured damping force via the FEM simulation data. Figure 10 qualitatively compares them.

Comparing the experimental and numerical model data, it is confirmed that the behaviour of both models is similar. Figure 10 proves that the increase in force is proportional to the excitation frequency. A significant point noted here is that the analytical model curve is smooth, whereas the experimental mode has some irregularities even though it is increasing proportionally. The irregular curve shape from 0.6hz to 0.9hz occurs due to the shear thickening of MR fluid, where MR fluid viscosity increases under shear loading.

Finally, it is highlighted through this investigation that with increased excitation frequency, with higher frequencies shear thickening phenomenon occurs in the MR damper, and the corresponding damping force also increases, which relates to higher velocity and damping coefficient.

TABLE 4. Total Damping force procured through investigation

Frequency (Hz)	Damping Force For Numerical (N)	Damping Force for Experimental (N)
0.1	171.3267	175.9103
0.2	183.358	185.3950
0.3	191.6985	195.8292
0.4	198.4517	202.6527
0.5	200.6951	204.2349
0.6	203.6824	205.3156
0.7	207.3215	209.7016
0.8	215.1295	227.1423
0.9	230.3655	224.8602
1	249.2398	252.7765

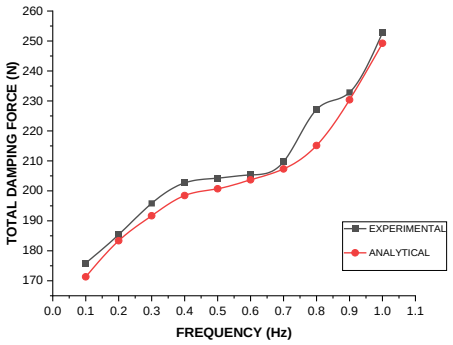

Figure 10. Relationship of force and frequency plot for various frequency

5. CONCLUSION

The most popular fluids in MR dampers for achieving variable damping coefficient are MR fluids. For the manufactured MR damper, FEM modelling has been done using the COMSOL platform. The magnetic flux density values obtained from the COMSOL study were used to calculate the overall damping force. Then, experimental damping force is achieved by running tests on the prototyped fabricated MR damper using the MTS servo-hydraulic machine with various excitation frequencies. When these two modelling results are compared, it is confirmed that the overall damping forces produced numerically and experimentally are almost equal with an error margin (1N-5N) which is negligible, throughout a broad range of excitation frequencies. It can be seen from the different graphical findings that the damper experiences a total maximum dampening force of 252.7768 N and 249.2398N at 1hz for FEM and the Experimental model respectively.

This research concludes that the Finite Element Model accurately captures the behaviour of the fabricated MR damper. The methodology used in this paper's study is sufficient for controlling and designing an MR damper. The findings of this study will aid designers in producing MR dampers that are more dependable and efficient, as well as in predicting the damping force within the engineering analysis's allowable error.

6. REFERENCES

1. Chen, E., Si, C. and Liu, J., "Experimental study of magneto-rheological materials and its damper dynamic characteristics", in 2010 Sixth International Conference on Natural Computation, IEEE. Vol. 1, (2010), 278-281.
2. Ferdaus, M.M., Rashid, M.M., Shanta, M., Tamanna, N. and Hasan, M.H., "Experimental investigation on magnetorheological damper's characterization", in Advanced Materials Research, Trans Tech Publ. Vol. 1115, (2015), 476-479.
3. Kasprzyk, J., Wyrwał, J. and Krauze, P., "Automotive mr damper modeling for semi-active vibration control", in 2014 IEEE/ASME international conference on advanced intelligent mechatronics, IEEE., (2014), 500-505.
4. Gudmundsson, K., Jonsdottir, F. and Thorsteinsson, F., "A geometrical optimization of a magneto-rheological rotary brake in a prosthetic knee", ***Smart materials and Structures***, Vol. 19, No. 3, (2010), 035023. doi: 10.1088/0964-1726/19/3/035023.
5. Powell, L.A., Hu, W. and Wereley, N.M., "Magnetorheological fluid composites synthesized for helicopter landing gear applications", ***Journal of Intelligent Material Systems and Structures***, Vol. 24, No. 9, (2013), 1043-1048. doi: 10.1177/1045389X13476153.
6. Nguyen, Q., Choi, S.-B. and Woo, J., "Optimal design of magnetorheological fluid-based dampers for front-loaded washing machines", ***Proceedings of the Institution of Mechanical Engineers, Part C: Journal of Mechanical Engineering Science***, Vol. 228, No. 2, (2014), 294-306. doi: 10.1177/0954406213485908.
7. Motra, G.B., Mallik, W. and Chandiramani, N.K., "Semi-active vibration control of connected buildings using magnetorheological dampers", ***Journal of Intelligent Material Systems and Structures***, Vol. 22, No. 16, (2011), 1811-1827. doi: 10.1177/1045389X11412640.
8. Oh, J.-S., Shin, Y.-J., Koo, H.-W., Kim, H.-C., Park, J. and Choi, S.-B., "Vibration control of a semi-active railway vehicle suspension with magneto-rheological dampers", ***Advances in Mechanical Engineering***, Vol. 8, No. 4, (2016), 1687814016643638. doi: 10.1177/1687814016643638.
9. Martynowicz, P. and Szydło, Z., "Wind turbine's tower-nacelle model with magnetorheological tuned vibration absorber", in Proceedings of the 14th international Carpathian control conference (ICCC), IEEE., (2013), 238-242.
10. Srinivasan, S., Kebede, S. and Chandramohan, S., "Performance evaluation of magnetorheological damper valve configurations using finite element method", ***International Journal of Engineering, Transactions B: Applications*** Vol. 30, No. 2, (2017), 303-310. doi: 10.5829/idosi.ije.2017.30.02b.18.
11. Daniel, C., Hemalatha, G., Sarala, L., Tensing, D. and Sundar Manoharan, S., "Seismic mitigation of building frames using magnetorheological damper", ***International Journal of Engineering***, ***Transactions B: Applications,*** Vol. 32, No. 11, (2019), 1543-1547. doi: 10.5829/ije.2019.32.11b.05.
12. Seid, S., Chandramohan, S. and Sujatha, S., "Design and evaluation of a magnetorheological damper based prosthetic knee", ***International Journal of Engineering***, ***Transactions A***: ***Basics***, Vol. 32, No. 1, (2019), 146-152. doi: 10.5829/ije.2019.32.01a.19.
13. Hou, Z.N., Feng, Z.M., Hu, H.G. and Wu, G.B., "Experimental study on performance characteristics of magnetorheological damper", in Applied Mechanics and Materials, Trans Tech Publ. Vol. 37, (2010), 439-443.
14. Wu, W. and Cai, C., "Experimental study of magnetorheological dampers and application to cable vibration control", ***Journal of Vibration and Control***, Vol. 12, No. 1, (2006), 67-82. doi: 10.1177/1077546306061128.
15. Ganesha, A., Patil, S., Kumar, N. and Murthy, A., "Magnetic field enhancement technique in the fluid flow gap of a single coil twin tube magnetorheological damper using magnetic shields", ***Journal of Mechanical Engineering and Sciences***, Vol. 14, No. 2, (2020), 6679-6689.
16. Wani, Z.R., Tantray, M. and Farsangi, E.N., "Investigation of proposed integrated control strategies based on performance and positioning of mr dampers on shaking table", ***Smart Materials and Structures***, Vol. 30, No. 11, (2021), 115009.

17. Wani, Z.R., Tantray, M. and Farsangi, E.N., "In-plane measurements using a novel streamed digital image correlation for shake table test of steel structures controlled with mr dampers", ***Engineering Structures***, Vol. 256, (2022), 113998.
18. Cruze, D., Gladston, H., Farsangi, E.N., Banerjee, A., Loganathan, S. and Solomon, S.M., "Seismic performance evaluation of a recently developed magnetorheological damper: Experimental investigation", ***Practice Periodical on Structural Design and Construction***, Vol. 26, No. 1, (2021), 04020061.
19. Cruze, D., Gladston, H., Farsangi, E.N., Loganathan, S., Dharmaraj, T. and Solomon, S.M., "Development of a multiple coil magneto-rheological smart damper to improve the seismic resilience of building structures", ***The Open Civil Engineering Journal***, Vol. 14, No. 1, (2020). doi.
20. Abdeddaim, M., Djerouni, S., Ounis, A., Athamnia, B. and Farsangi, E.N., "Optimal design of magnetorheological damper for seismic response reduction of base-isolated structures considering soil-structure interaction", in Structures, Elsevier. Vol. 38, (2022), 733-752.
21. Rashid, Z., Tantray, M. and Noroozinejad Farsangi, E., "Acceleration response-based adaptive strategy for vibration control and location optimization of magnetorheological dampers in multistoried structures", ***Practice Periodical on Structural Design and Construction***, Vol. 27, No. 1, (2022), 04021065.
22. Wani, Z.R., Tantray, M. and Farsangi, E.N., "Shaking table tests and numerical investigations of a novel response-based adaptive control strategy for multi-story structures with magnetorheological dampers", ***Journal of Building Engineering***, Vol. 44, (2021), 102685.
23. Wani, Z.R., Tantray, M.A., Iqbal, J. and Farsangi, E.N., "Configuration assessment of mr dampers for structural control using performance-based passive control strategies", ***Structural Monitoring and Maintenance***, Vol. 8, No. 4, (2021), 329-344.
24. Sharma, S.V., Hemalatha, G. and Ramadevi, K., "Analysis of magnetic field-strength of multiple coiled mr-damper using comsol multiphysics", ***Materials Today: Proceedings***, (2022). doi: 10.1016/j.matpr.2022.05.279.
25. Jolly, M. and Sun, J., "Lord corporation, thomas lord research center", ***Smart Structures and Materials: Passive Damping***, (1994), 194.
26. Guo, N., Du, H. and Li, W., "Finite element analysis and simulation evaluation of a magnetorheological valve", ***The International Journal of Advanced Manufacturing Technology***, Vol. 21, No. 6, (2003), 438-445.
27. Dixon, J.C., "The shock absorber handbook, John Wiley & Sons, (2008).
28. Carlson, J.D., Catanzarite, D. and St. Clair, K., "Commercial magneto-rheological fluid devices", ***International Journal of Modern Physics B***, Vol. 10, No. 23n24, (1996), 2857-2865.
29. Xu, Z.-D., Jia, D.-H. and Zhang, X.-C., "Performance tests and mathematical model considering magnetic saturation for magnetorheological damper", ***Journal of Intelligent Material Systems and Structures***, Vol. 23, No. 12, (2012), 1331-1349.
30. Wang, X. and Gordaninejad, F., "Dynamic modeling of semi-active er/mr fluid dampers", in Smart structures and materials 2001: Damping and isolation, SPIE. Vol. 4331, (2001), 82-91.
31. Jiang, X., Wang, J. and Hu, H., "Designing and modeling of a novel magneto-rheological fluid damper under impact load", in 3rd International Conference on Mechanical Engineering and Mechanics, Beijing, China., (2009), 203-207.

Persian Abstract

چکیده

این مقاله طراحی یک دمپر مغناطیسی (MR) را ارائه می‌کند که شامل آرایش پیستون و سیلندر است. این مطالعه یک مدل سه بعدی را بر اساس مفهوم روش المان محدود (FEM) در COMSOL Multiphysics برای تجزیه و تحلیل و بررسی ویژگی‌های دمپر MR ایجاد کرد. یک نمونه اولیه از دمپر MR بر اساس مدل FEM ساخته می شود و با استفاده از Servo-Hydraulic MTS تحت یک سری آزمایش قرار گرفته است. حداکثر و حداقل نیرو، N۱۷۱.۵۲۳۵ و N۲۴۹.۲۷۴۹، به ترتیب در Hz۰.۱ و Hz۱، برای مدل FEM اندازه گیری شد. مدل ساخته شده نتایج مشابهی را در ۰.۱ هرتز و ۱ هرتز، با حداکثر و حداقل نیروهای N۱۷۵.۹۱۰۳ و N۲۵۲.۷۷۶۵ به دست آورد. مقایسه این دو تحلیل مدل نشان می‌دهد که مدل مبتنی بر FEM به دقت رفتار تجربی دمپر MR را از نظر نیروی میرایی آن به تصویر می‌کشد، اگرچه تغییرات جزئی وجود دارد. یافته‌های این مقاله برای طراحان در ایجاد دمپرهای MR که کارآمدتر و قابل اعتمادتر هستند و همچنین در پیش‌بینی ویژگی‌های نیروی میرایی آنها مفید خواهد بود.